Project: 549

Project Title: Modellierung von Klimaeffekten von Mittel- und Südamerikanischen Vulkanen

"Modelling the climate effects of Middle and South American volcanoes"

Project Leader and Team: Kirstin Krüger (formerly IFM-GEOMAR Kiel, now at University of Oslo), Claudia Timmreck (MPI-M, Hamburg), Matthew Toohey (GEOMAR Kiel), and Doreen Metzner (IFM-GEOMAR, Kiel)

Report Period: 1.1.2010 - 01.01.2017

The DKRZ project 549 "Modelling the climate effects of Middle and South American volcanoes" ran from 01.01.2010 until 01.01.2017. It was originally set up within the "Sub project C5: Climate modelling" of the SFB 574 project on "Volatiles and Fluids in Subduction Zones: Climate Feedback and Trigger Mechanisms for Natural Disasters" (July 2008 - June 2012) at IFM-GEOMAR, later called GEOMAR, in Kiel (https://sfb574.geomar.de). Our successful research work continued beyond the SFB 574 project time into 2016. Below you find a chronicle summary of our highlight results followed by a list of project relevant publications.

2010:

In a similar approach as were done for the Toba super eruption 74 ka ago (Timmreck et al., 2010) we modelled the climate effect of Middle and South American volcanoes. We first calculated and simulated the radiative forcing of explosive volcanic eruptions with different SO_2 strength using parameterizations from available literature and the aerosol-climate model MAECHAM5/HAM with interactive microphysics and sulphur chemistry. The MAECHAM5/HAM simulations were run on Blizzard. As Figure 1 reveals, the relationship between volcanic SO_2 injection to the stratosphere and simulated Aerosol Optical Depth (AOD) is linear for small eruptions up to (<5 Mt SO_2), and non-linear for large eruptions (>5 Mt SO_2). In the same study by Metzner et al. (2014), we compiled a new radiative forcing data set for all available Central American Volcanic Arc (CAVA) eruptions of the last 200 ka, which was the key paper for the following modelling work within the DKRZ project 549. The calculations for the resulting paper by Metzner et al. were carried out during 2010, submitted 2011, published online 2012 (Metzner et al., 2014 published on paper).

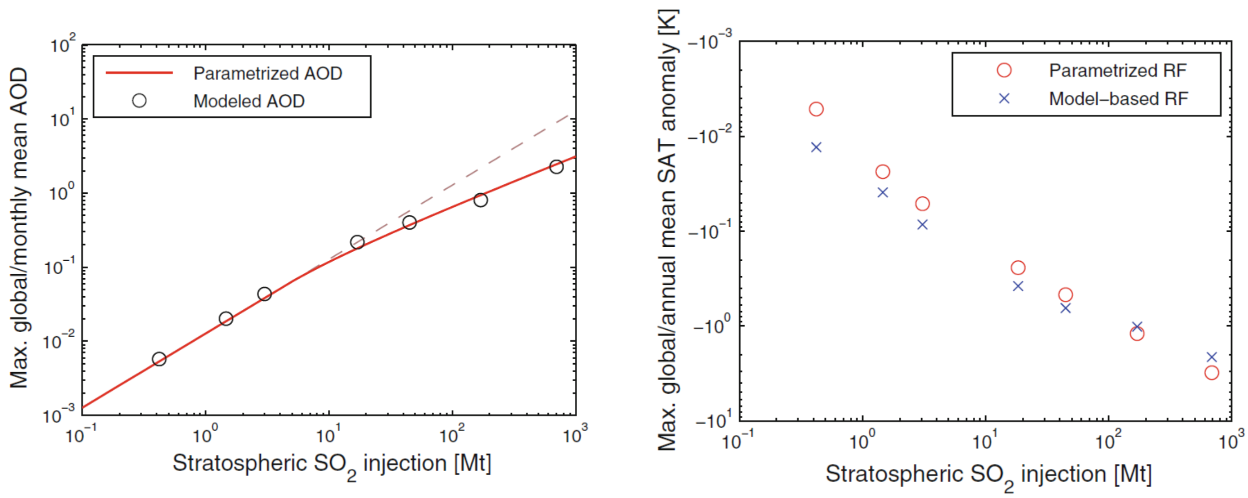

Figure 1: Left: Parameterized and modelled maximum global mean monthly mean AOD at a wavelength of 0.55 μm as a function of stratospheric SO_2 injection (Mt). Open circles show results from MAECHAM5-HAM simulations with selected SO_2 injections. The linear relationship used for SO_2 injections less than 4.9 Mt is extrapolated to higher SO_2 injections (dashed line) for comparison. Right: Maximum global mean annual mean surface air temperature (SAT) anomaly (K) calculated with CLIMBER-2 for different stratospheric SO_2 injections (Mt). Open red circles show results for the simulations forced with parametrized Radiative Forcing (RF); the blue crosses represent simulations forced with model-based RF (Metzner et al. 2014).

2011:

In the following MAECHAM5 simulations for the CAVA, we investigated the climate influence of large tropical eruptions depending on the season of the eruption (Toohey et al. 2011). In this study we concentrated on one large (17 Mt SO_2, Pinatubo size; experiment E17) and one extremely large (700 Mt SO_2, Los Chocoyos 84 ka; experiment E700) eruption. In sensitivity studies we investigated the influence of the time of the eruption (season) on the radiative forcing. The model results showed that the season of the eruption has a significant impact on the AOD and the clear-sky solar radiative forcing flux anomalies, independent of the strength of the eruption. Changes in the all-sky solar flux are however only relevant for the extreme large eruption E700. As one can clearly see in Figure 2, the transport of sulphate aerosol, and hence the spatial structure of the AOD, are sensitive to the different strength and seasons of the eruptions. In particular, the amount of sulphate aerosol reaching the polar latitudes is quite sensitive to the eruption season and magnitude. This interesting result led a follow up model paper on the volcanic sulphur deposition to the polar ice sheets in the DKRZ project 549.

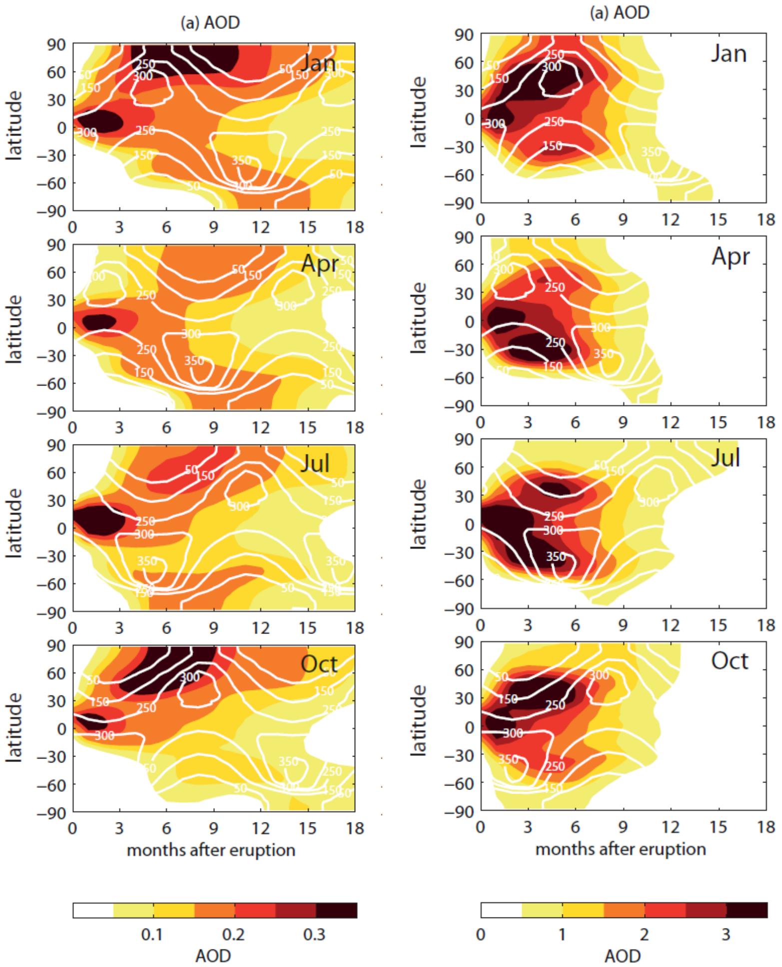

Figure 2: Zonal mean, monthly mean 0.55 µm aerosol optical depth for (left panel) 17 Mt SO_2 injection and (right) 700 Mt SO_2 injection eruptions in January, April, July and October based on MAECHAM5-HAM. White contours in column show climatological surface clear-sky shortwave radiation: visual contrast between colour shading and white contours is used to highlight climatological radiative flux at timing of large AOD. All anomalies shown are ensemble mean differences from a control run, and are significant at the 95 % confidence level (Toohey et al., 2011).

2012:

Based on the radiative forcing from the MAECHAM5-HAM E700 experiments for the Los Chocoyos 84 ka (LCY) eruption in Guatemala we ran MPI-ESM T31/L19 simulations for a June eruption to test the climate response including a fully coupled ocean. The simulations were set up from a 2000 year control run with unperturbed pre-industrial (800 CE (common era) conditions using five different El Niño Southern Oscillation (ENSO) initial conditions, as done in Timmreck et al. (2012), implementing the volcanic forcing which last approximately 4 years. The experiments were run for 200 years without additional forcing, which allows for an assessment of the simulated centennial-scale climate impacts of the Los Chocoyos eruption.

An almost global surface cooling is simulated in the first two years after the eruption with only some regional warming mainly in the Southern Ocean (Figure 3). Concentrating on the Southern

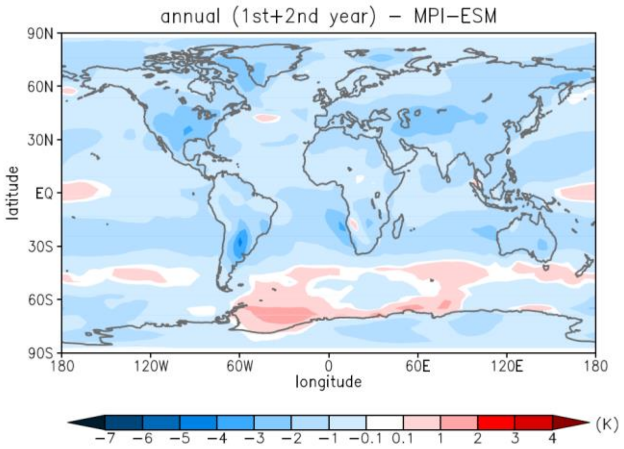

Figure 3: Surface annual mean temperature anomalies (K) for the first two years after the Los Chocoyos eruption simulated with the MPI-ESM.

(a) (b)

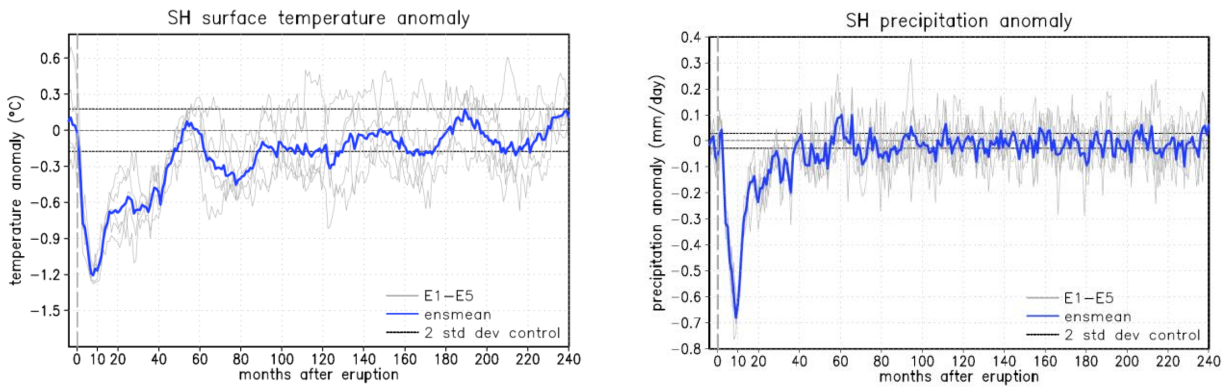

Figure 4: Simulated SH monthly mean anomalies for the first 20 years, based on MPI-ESM. Shown are the ensemble mean (blue line) and the different runs (grey lines) for (a) the surface temperature (°C), and (b) the precipitation (mm/day). The horizontal dashed lines denote the 2σ (standard deviation) thresholds.

Hemisphere (SH) with the maximum hemispheric volcanic forcing, negative monthly-mean surface temperature and precipitation anomalies are investigated in Figure 4. With a maximum cooling of 1.2° C after 6 - 7 months and a reduction in precipitation up to 0.7 mm/day after 8 - 9 months, the ensemble-mean anomalies exceed the range of internal variability for about 7 and 5 years, respectively. The relaxation time of the surface temperature anomalies is longer than the stratospheric one, which may indicate the relaxation of damped ocean response. Note that the within-ensemble spread is hardly discernible in SH stratospheric temperatures, but clearly apparent in surface anomalies, in particular for temperatures one year after the eruption. This indicates the large internal variability due to ENSO becoming most clearly in the surface temperature anomalies.

Consistent with the temperature changes in the stratosphere (not shown), the largest zonal-mean zonal wind anomalies (14 m/s) are detected in the lower to middle stratosphere between 30°S and 60°S according to the largest temperature gradient (Figure 5).

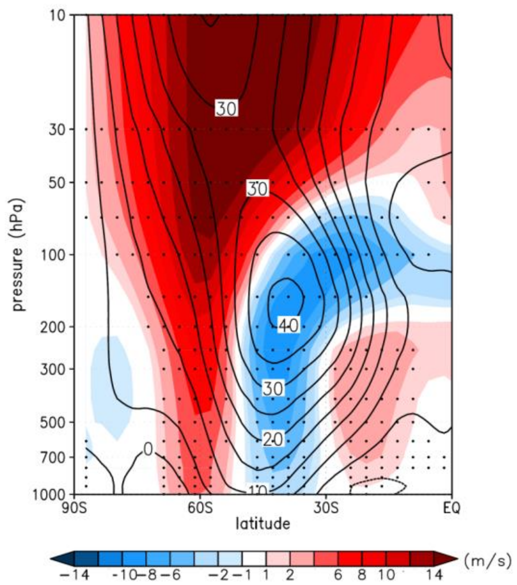

Figure 5: SH zonally averaged zonal wind anomalies (m/s; shaded) for the first year after the eruption, based on MPI-ESM. The climatology is given by the contour lines at which dashed lines indicate negative values; the interval is 5 m/s. The black dots denote significant anomalies.

Regarding the stratospheric westerly wind anomalies of more than 14 m/s at about 50°S to 60°S, these anomalies correspond to zonal wind absolute velocities exceeding 40 m/s. The stratospheric signal of significantly enhanced westerlies extends downward affecting the lower tropospheric levels. A significant amplification of near-surface winds in the high to mid-latitudes is accompanied with a weakening equatorward between 30˚S and 50°S, which corresponds to a poleward displacement of the westerly winds, i.e., of the subtropical jet stream. The post-eruption circulation anomaly pattern resembles the dipole pattern typically associated with a positive Southern Annular Mode (SAM) phase.

A poleward shift of the zonal-mean zonal wind stress is simulated during the first post-eruption year (Figure 6 left), which results in maximum values occurring about 55˚S, i.e., in the region of the Antarctic Circumpolar Current (about 40˚S to 60˚S; Figure 6 right). Following, an acceleration of the zonal current in the Southern Ocean at 60°S is simulated lasting for more than 30 years after the eruption. Significant anomalies extend towards deeper ocean layers, and ocean current anomalies up to 0.4 cm/s are found down to depths of 2000 m.

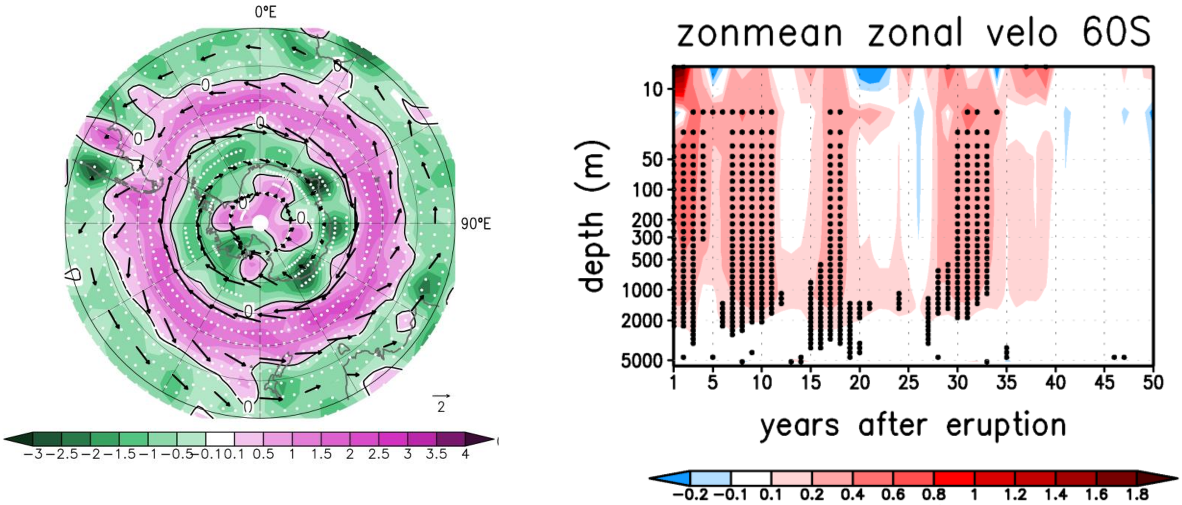

Figure 6: Left: Polar stereographic map showing SH (30˚S to 90˚S) surface wind stress (N/m^2) and wind (m/s) anomalies for the first year after the eruption. Right: Zonal mean zonal ocean velocity anomalies (cm/s) at 60˚ S for 50 years after the eruption. Based on MPI-ESM; significances are indicated by the white and black dots.

This coupled climate model work was part of the PhD thesis by Doreen Metzner (SFB 574, IFM-GEOMAR, Kiel), which was nearly completed in 2012, but unfortunately never submitted by the PhD candidate to University of Kiel.

Stephanie Gleixner (2012) investigated in her Master thesis the response of the SAM to volcanic forcing in MPI-ESM historical simulations produced as part of the 5th Climate Model Intercomparison Project (CMIP5), which include historical eruptions such as those of Mt. Pinatubo (1991), El Chichón (1982) and Krakatau (1883). Like previous generation CMIP3 models, the MPI-ESM displayed a positive stratospheric SAM response to Pinatubo and El Chichón, in contrast to the negative post-eruption SAM seen in observations. Surface SAM response to the eruptions is not significant, consistent with the results of the MAECHAM5-HAM simulations discussed below (see 2014 Section).

2013:

In 2013, computations within Project 549 focussed on expanding the ensemble of volcanic simulations with the MAECHAM5-HAM model configuration. A major focus was on the simulated deposition of volcanic sulphate to the Antarctic and Greenland ice sheets. In the study of Toohey et al. (2013), an ensemble of 70 volcanic simulations was assessed, with SO_2 injections to the stratosphere ranging from 7.5 to 700 Mt, with eruptions initiated in January and July. Modelled sulphate deposition flux to Antarctica showed excellent spatial correlation with ice core-derived estimates (Figure 7), although the comparison suggests the modelled flux to the ice sheets is 4-5 times too large.

Greenland and Antarctic deposition efficiencies (the ratio of sulphate flux to each ice sheet to the maximum hemispheric stratospheric sulphate aerosol burden) were found to vary as a function of the magnitude and season of stratospheric sulphur injection. Changes in simulated sulphate deposition for large SO_2 injections were connected to increases in aerosol particle size, which impact aerosol sedimentation velocity and radiative properties, the latter leading to strong dynamical changes including strengthening of the winter polar vortices, which inhibits the transport of stratospheric aerosols to high latitudes. The resulting relationship between Antarctic and Greenland volcanic sulphate deposition is nonlinear for very large eruptions, with significantly less sulphate deposition to Antarctica than to Greenland. MAECHAM5-HAM-simulated volcanic sulphate deposition was also compared to an extensive database of Antarctic ice core data (Sigl et al., 2014).

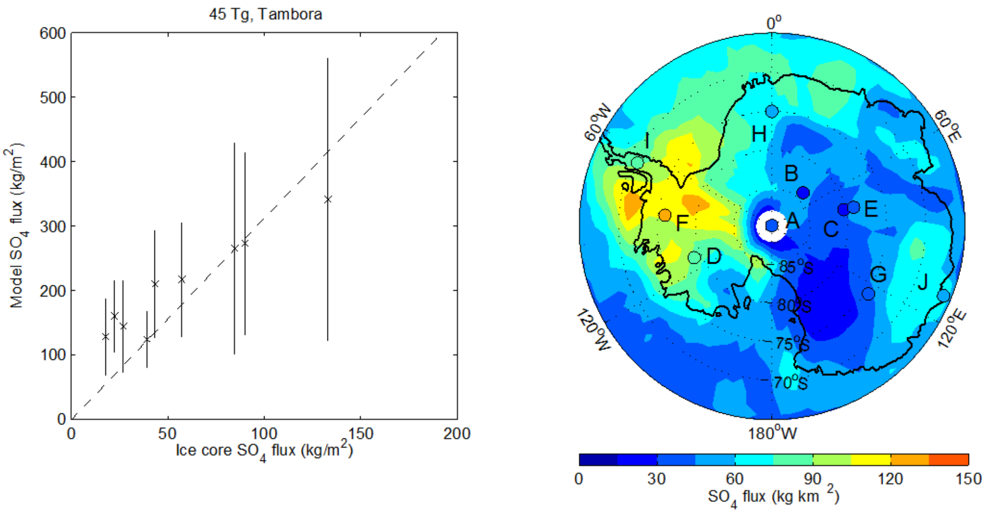

Figure 7: Comparisons of modelled versus measured Antarctic sulphate fluxes for Tambora ice core fluxes and 45 Mt SO_2 injection MAECHAM5-HAM experiment (Toohey et al., 2013).

2014:

In 2014, computations within Project 549 were utilized to span a wide range of stratospheric sulphur injections based on MAECHAM5-HAM simulations of CAVA eruptions, to investigate the relationship between eruptive sulphur release and the SAM response. Figure 8 shows the increase in first year average SAM with increasing stratospheric sulphur injection, for both the lower stratosphere and at the surface. Increases in post-eruption SAM are roughly linear for small to medium eruptions, but by simulating a range of eruptions up to that of Los Chocoyos, one can see the relationship is non-linear, and instead shows an asymptotic behaviour for the larger eruptions. By comparing the simulated volcanic SAM response to the natural SAM variability, one can interpolate to find the eruptive stratospheric sulphur injection needed to produce a significant SAM response. We find that a stratospheric SO_2 injection of 16 Mt is needed to produce a significant stratospheric response, but a much larger injection, 91 Mt, is needed to produce a sig-

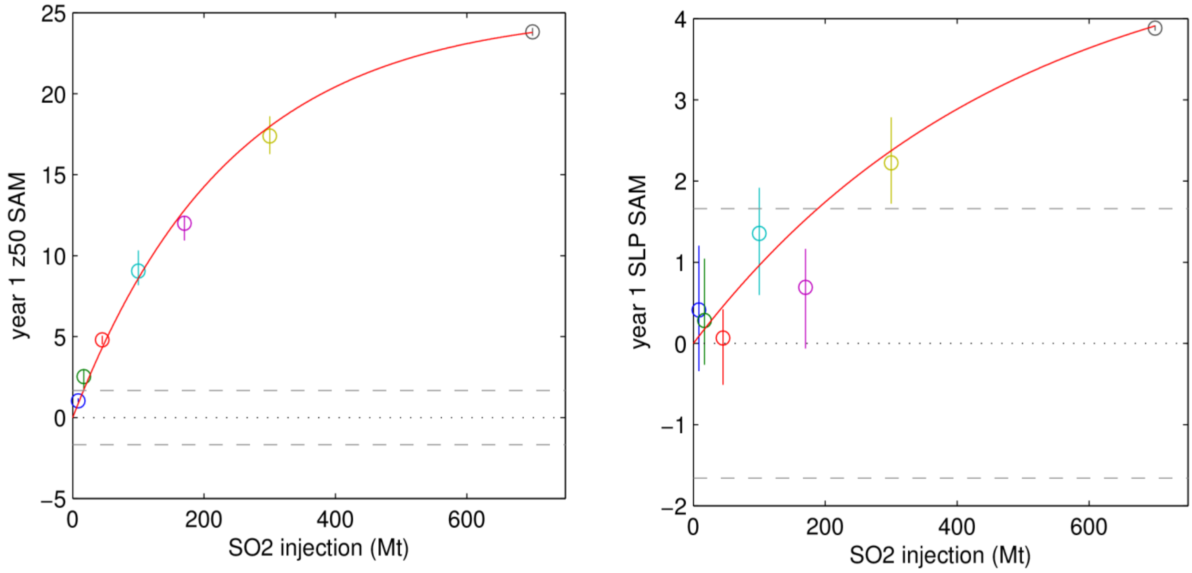

Figure 8: SAM response for the first post-volcanic year for the lower stratosphere (50 hPa, left panel) and at the surface (sea level pressure, right panel) as a function of injected SO_2 mass; based on MAECHAM5-HAM simulations. SO_2 mass injections of 16 and 91 Mt are found to lead to SAM signals just larger than the 2-sigma natural variability in the stratosphere and at the surface, respectively.

nificant response at the surface. The results are planned to be submitted in 2017 (Krüger and Toohey, in preparation).

2015 and 2016:

Substantial progress was achieved in 2015 (model runs and analysis) and in 2016 (analysis and writing paper) by investigating the climate anomalies of the decades following 536 CE, which is speculated to be connected to the Ilopango eruption of Central America.

Volcanic activity in and around the year 536 CE led to severe cold, famines, and has been speculatively linked to large-scale societal crises around the globe. Using the MAECHAM5-HAM coupled aerosol-climate model, with eruption parameters constrained by recently re-dated ice core records and historical observations of the aerosol cloud, we have reconstructed the radiative forcing resulting from a sequence of two unknown major volcanic eruptions in 536 and 540 CE (Fig 9). We estimate that the decadal-scale Northern Hemisphere (NH) extra-tropical radiative forcing from this volcanic “double event” was larger than that of any period in existing reconstructions of the last 1200 years.

Simulations of the time period with the MPI-ESM, including the volcanic forcing, show peak NH mean temperature anomalies reaching more than -2°C (Fig. 10), and show agreement with the limited number of available maximum latewood density temperature reconstructions. The simulations also produce decadal-scale anomalies of Arctic sea ice. The simulated cooling is interpreted in terms of probable impacts on agricultural production in Europe, and implies a high likelihood of multiple years of significant decreases in crop production across Scandinavia in the years following 536 CE, supporting the theory of a connection between the 536 and 540 eruptions and evidence of societal crisis dated to the mid-6th century.

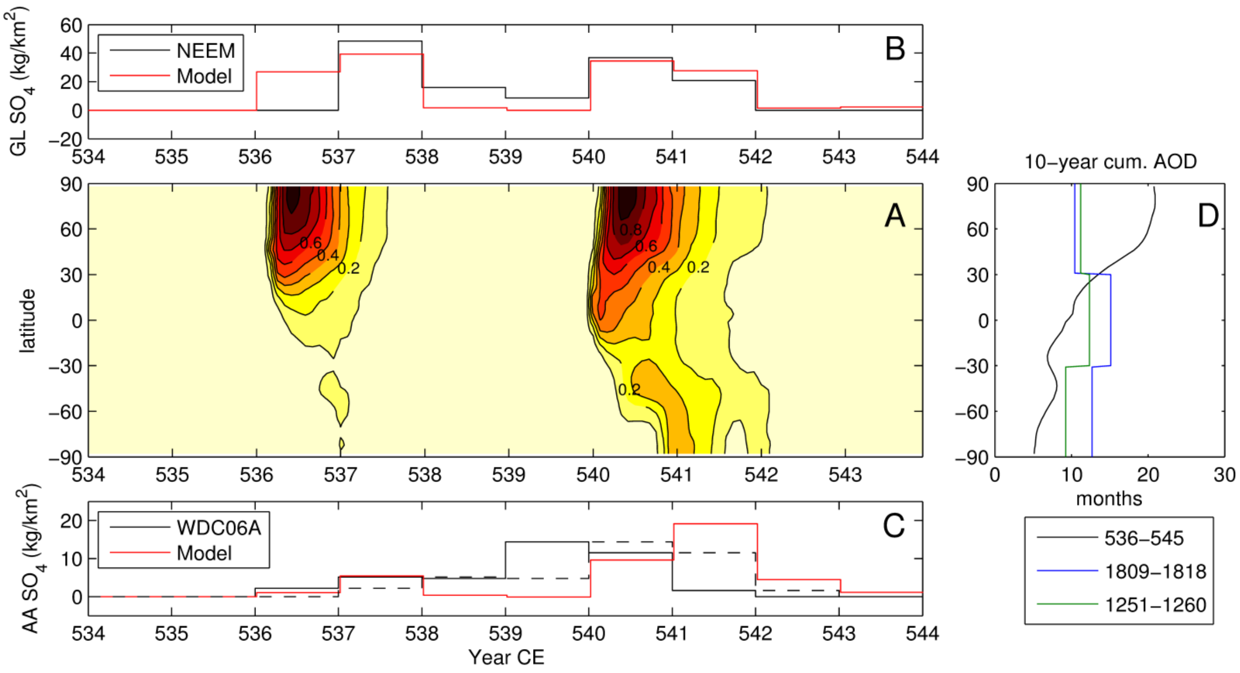

Figure 9: Volcanic radiative forcing 536-544 CE estimated from ice core records. (A) Reconstructed zonal mean aerosol optical depth at 550 nm from MAECHAM5-HAM and used as radiative forcing in MPI-ESM simulations. Time series of annual volcanic sulphate deposition from the (B) Greenland NEEM(-2011-S1) ice core (Sigl et al., 2012) and (C) Antarctic WDC06A ice core (Sigl et al., 2012) compared to bias-corrected sulphate flux to Greenland and Antarctica in MAECHAM5-HAM simulations (Toohey et al., 2013). Antarctic ice core flux shifted by +1 year is shown by dashed black line. (D) Decadal cumulative AOD, compared to that of the two largest NH decadal forcings of the volcanic AOD reconstruction of (Crowley and Unterman, 2013). (Toohey et al., 2016)

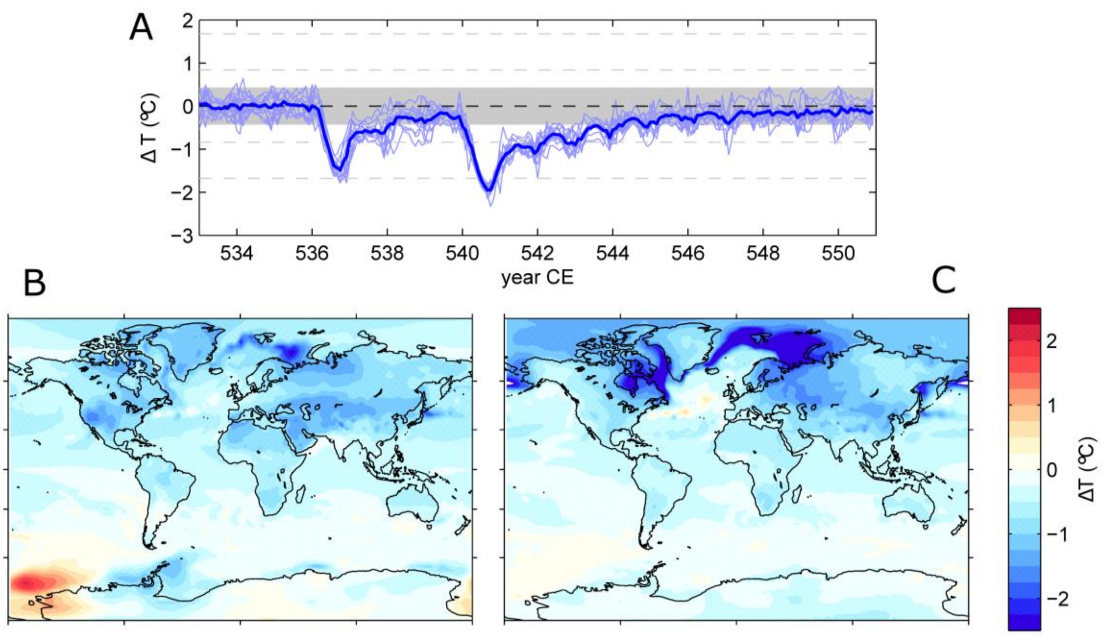

Figure 10: Surface temperature anomalies simulated by the MPI-ESM. (A) Timeseries of Northern Hemisphere mean monthly mean surface temperature anomalies: individual ensemble members shown in light blue, ensemble mean in thick blue. Gray shading show the ±2σ variability of the control run, dashed grey lines show the ±4σ and ±8σ variability levels. Global maps of the 536-545 CE decadal mean boreal (B) summer and (C) winter mean temperature anomalies. (Toohey et al., 2016)

Overall Results and Outlook:

Within the DKRZ project 549 "Modelling the climate effects of Middle and South American volcanoes" running from 1.1.2010 to 01.01.2017, we have successfully investigated the climate effects of Middle and South American volcanic eruptions of the past 200 ka. We used different MPI models on Blizzard to better understand the physical process as well as the climate response of Middle and South American volcanic eruptions in more detail. Significant project results have been achieved, which are reflected by 18 project and project-related peer reviewed articles, theses, reports and books published between 2010 and 2016. Due to external changes of model developments, the complex chemistry climate model HAMMOZ was not ready for use and to simulate the chemical effects of large sulphur and halogen rich eruptions. However, three publications were written and published on the potential chemical effects of these large paleo eruptions on ozone (Kutterolf et al., 2013/2015; Krüger et al., 2015). Currently the chemical ozone effects of large tropical volcanic eruptions are investigated in two follow up projects: i) Within the second phase of the BMBF MIKLIP project ALARM-II by Claudia Timmreck and Hauke Schmidt (MPI) and ii) through the PhD student Hans Brenna at University of Oslo supervised by Kirstin Krüger investigating the ozone impact by the Middle and South American eruptions.

Overall, the 549 project successfully led to synergy effects between different disciplines of volcanology, atmospheric physics and chemistry and climate as well as it led to follow up funded national and international projects.

Project* and Project-Related References (Total 18)

Peer-review Publications (10):

Kutterolf, S, T. Hansteen, K. Appel, A. Freundt, K. Krüger, W. Peréz, and H. Wehrmann, The combined Bromine and Chlorine release from large explosive volcanic eruptions: a threat to stratospheric ozone?, GEOLOGY, 41(6); 707–710, doi: 10.1130/G34044.1, 2013.

Kutterolf, S., T. H.Hansteen, A. Freundt, H. Wehrmann, K. Appel, K. Krüger, W. Pérez, Bromine and chlorine emissions from Plinian eruptions along the Central American Volcanic Arc: From source to atmosphere, EPSL, Vol. 429, 234-246, 2015.

Krüger, K., Kutterolf, S., T.H., Hansteen, Chapter 16: Halogen release from Plinian eruptions and depletion of stratospheric Ozone, Volcanism and global environmental change, Cambridge University Press, isbn: 9781107058378, Ed. A. Schmidt et al., PP. 244-259, 2015.

*Metzner, D., S. Kutterolf, M. Toohey, C. Timmreck, U. Niemeier, A. Freundt, K. Krüger, Radiative forcing and climate impact resulting from SO2 injections based on a 200,000 year record of Plinian eruptions along the Central American Volcanic Arc, Int J Earth Sci, DOI 10.1007/s00531-012-0814-z, 103(7), 2063-2079, (online already 2012) 2014.

*Timmreck, C., H. ‐ F. Graf, S. J. Lorenz, U. Niemeier, D. Zanchettin, D. Matei, J. H. Jungclaus, and T. J. Crowley, Aerosol size confines climate response to volcanic super ‐ eruptions, Geophys. Res. Lett., 37, L24705, doi:10.1029/ 2010GL045464, 2010.

*Timmreck, C., Graf, H.-F., Zanchettin, D., Hagemann, S., Kleinen, T. and Krüger, K., Climate response to the Toba super-eruption: Regional changes, Quaternary International, 258, 30-44, 2012.

*Toohey, M., Krüger, K., Niemeier, U., and Timmreck, C.: The influence of eruption season on the global aerosol evolution and radiative impact of tropical volcanic eruptions, Atmos. Chem. Phys., 11, 12351-12367, doi:10.5194/acp-11-12351-2011, 2011.

*Toohey, M., Krüger, K. and Timmreck, C.: Volcanic sulfate deposition to Greenland and

Antarctica: A modeling sensitivity study, Journal of Geophysical Research: Atmospheres, 118(10), 4788–4800, doi:10.1002/jgrd.50428, 2013.

Toohey, M., Krüger, K., Sigl, M., Stordal, F. and Svensen, H.: Climatic and societal impacts of a volcanic double event at the dawn of the Middle Ages, Clim. Change, doi:10.1007/s10584-016-1648-7, 2016.

Sigl, M., J.R. McConnell, M. Toohey, M. Curran, S.B. Das, R. Edwards, E. Isaksson, K. Kawamura, K. Krüger, L. Layman, O. Maselli, Y. Motizuki, D. Pasteris, Rewriting the history of volcanic forcing during the Common Era using new ice cores, Nature Climatic Change, 10.1038/nclimate2293, 2014.

Theses (3):

*Gleixner, S. (2012) Southern Annular Mode response to volcanic eruptions in the MPI-ESM, Master thesis, Christian-Albrechts-University Kiel, 94 pp., supervised by Kirstin Krüger.

*Zander, S. (2010), Die Auswirkung von Vulkaneruptionen auf die atmosphärische Zirkulation in Abhängigkeit von der Ausbruchstärke", Bachelor thesis, Christian-Albrechts-University Kiel, 55 pp., supervised by Kirstin Krüger.

*Scheef, H. (2010), Der Einfluss von sehr starken Vulkaneruptionen auf die Nordatlantische und Arktische Oszillation im MAECHAM5-Modell", Bachelor thesis, Christian-Albrechts-University Kiel, 51 pp., supervised by Kirstin Krüger.

Books and Reports (5):

Butchart, N, A. Charlton-Perez, I., Cionni , S.C., Hardiman, Krüger, K. et al., Chapter 4: Stratospheric Dynamics (SPARC CCMVal Report on the Evaluation of Chemistry-Climate Models), SPARC No. 5, WCRP-132, WMO/TD-No. 1526, P. 109-148, 2010.

Manzini, E., et al., C. Timmreck, M. Toohey, S. Yoden, Chapter 8: Natural Variability of Stratospheric Ozone, (SPARC CCMVal Report on the Evaluation of Chemistry-Climate Models), SPARC No. 5, WCRP-132, WMO/TD-No. 1526, P. 109-148, 2010.

Montzka, S., S. Reimann, S. O'Doherty, A. Engel, K. Krüger, and W.T., Sturges, Chapter 1: Ozone-Depleting Substances (ODSs) and Related Chemicals, "Scientific Assessment of Ozone Depletion: 2010", World Meteorological Organization, Geneva, Switzerland, PP. 112, 2011.

Zierul, S., und K. Krüger, "Klima - Das Jahr ohne Sommer", Beitrag zum Buch "Am Puls der Erde - Naturkatastrophen verstehen", Herausgeber: P. Linke, S. Zierul, B. Friedländer, B. Grundmann, Wachholtz Verlag, Seiten 154-171, 2012.

Zierul, S., and K. Krüger, "Climate – The year without summer“, Contribution to the book: Taking the earth’s pulse – Understanding Natural disasters, ed. by Linke, P., Zierul, S., Friedländer, B., and Grundmann, B. Wachholtz Verlag, Neumünster, 197 pp, 2013.